Lipidic Protic Ionic Liquid Crystals

Guilherme J. Maximo,[†] Ricardo J. B. N. Santos,[‡] José A. Lopes-da-Silva,[§] Mariana C. Costa,[‖] Antonio J. A. Meirelles,[†] and João A. P. Coutinho*,[‡]

[†] Laboratory of Extraction, Applied Thermodynamics and Equilibrium, School of Food Engineering, University of Campinas, 13083-862, Campinas, São Paulo, Brazil

[‡] CICECO, Chemistry Department, University of Aveiro, 3810-193, Aveiro, Portugal

[§] QOPNA, Chemistry Department, University of Aveiro, 3810-193, Aveiro, Portugal

[‖] School of Applied Sciences, University of Campinas, 13484-350, Limeira, São Paulo, Brazil

Ⓢ Supporting Information

ABSTRACT: Protic ionic liquids (PILs) based on lipidic compounds have a range of industrial applications, revealing the potential of oil chemistry as a sustainable basis for the synthesis of ionic liquids. PILs of fatty acids with ethanolamines are here disclosed to form ionic liquid crystals, and their mixtures with the parent fatty acids and ethanolamines display a lyotropic behavior. Aiming at characterizing their rheologic and phase behavior, four ethanolamine carboxylates and the mixtures used for their synthesis through a Brønsted acid—base reaction are investigated. Their phase diagrams present a complex multiphase profile, exhibiting lyotropic mesophases as well as solid—liquid biphasic domains with a congruent melting behavior. These PILs present a high self-assembling ability and a non-Newtonian behavior with yield stress in the liquid crystal mesophase. The appearance of lamellar and hexagonal structures, with probably normal and inverted configurations in the mixtures, due to the formation of the PILs is responsible for the high viscoelasticity and notable nonideality that is mainly ruled by hydrophobic/hydrophilic interactions. Considering their renewable origin, the formation of liquid crystalline structures, in addition to the non-Newtonian behavior and ionic liquids properties, and the mixtures here evaluated possess a great potential, and numerous applications may be foreseen.

KEYWORDS: Ionic liquid, Solid—liquid equilibrium, Fatty acid, Ethanolamine, Liquid crystal, Rheology
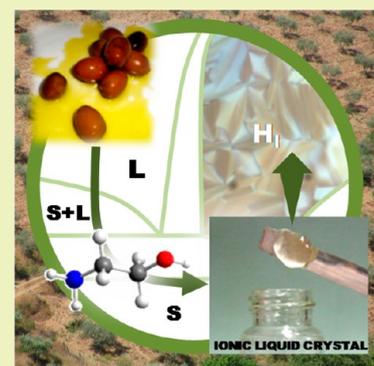
INTRODUCTION

More than a remarkable presence in the open literature during the past decade, ionic liquids and mesotherm (i.e., low melting) salts have long since been embodied in a large range of detergents, personal care cosmetic, pharmaceuticals, and chemical-marketed products. The interest for ionic liquids, salts with melting temperatures below 100 °C, was driven by their peculiar properties: negligible vapor-pressure, wide liquid-phase range, no or limited flammability, and a tunability that offers freedom for the design and optimization of chemical processes and product formulation. Such flexibility makes them also environmentally friendly by reducing the amount of byproducts in the industry.[1−3] A wide range of mesotherm salts based on fatty acids and their derivatives have been used long since as surfactants, and for many other purposes, without actually being recognized as ionic liquids. Protic ionic liquids (PILs) are produced through a Brønsted acid—base reaction (Figure 1) and, therefore, are capable of particular chemical interactions, including proton acceptance and proton donation. Because they are easily prepared, often from low-cost or even renewable reactants, PILs may be used in several industrial applications besides their use as surfactants, such as the design of electrolyte fuel cells, biocatalytic reactions, separation, and self-assembly processes.[4−6]

Addressing the claims of sustainable chemistry, the search for natural sources for the synthesis of ionic liquids with low environmental impacts seems to be more than a forthcoming trend; it seems to be an imperative demand.[7−9] In this way, taking into account the renewable aspects and relevance of several industrial sectors in the actual worldwide economic scenario, oil chemistry shows great potential to serve as a sustainable supplier of green chemicals. In fact, nowadays, the world production and consumption of vegetable oils is larger than 150 millions of tons.[10] Considering not only the refining process but also several other steps of the oil production chain, fatty acids emerge as a widely relevant byproduct. Being edible, chemically attractive due to the particular properties of their long carbon chain, and having low toxicity, they are widely used by the industry as the anion for the production of salts, and potentially of PILs, with properties tailored by choice of an appropriate proton acceptor.[11−15] Alkanolamines, such as
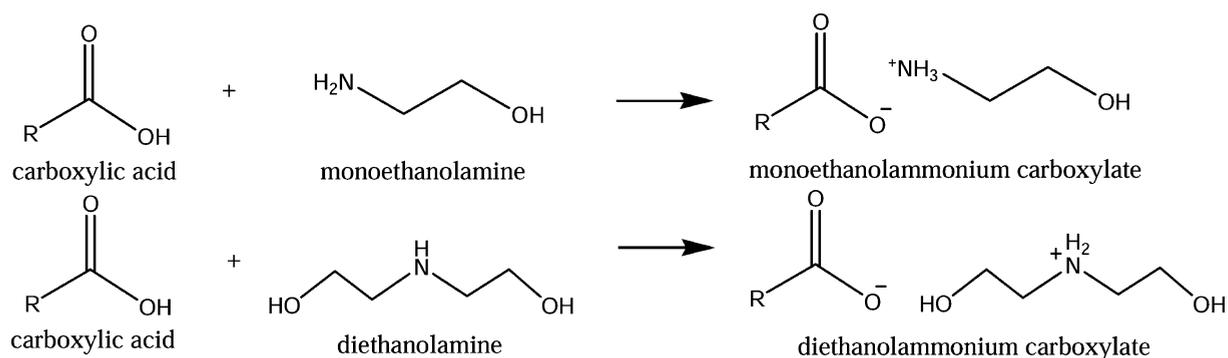
Figure 1. Brønsted acid–base reaction between a carboxylic acid and monoethanolamine or diethanolamine for the formation of a protic ionic liquid. R represents the alkylic moiety of the carboxylic acid.

mono-, di-, or tri-ethanolamine, are compounds naturally found in phospholipid biological membranes. They are often taken as the cation of the acid–base reaction with fatty acids to produce soaps, which are actually PILs, used in the formulation of industrial and hand cleaners, cosmetic creams, aerosol shave foams, and industrial lubricants due to their excellent emulsifying, thickening, and detergent ability in oil-in-water emulsions.[16−19] In particular, monoethanolamine oleate has long been embodied in the pharmaceutical industry. Approved by U.S. Food and Drug Administration (FDA), it acts as sclerosant agent when a diluted solution is administrated intravenously in the treatment of leg veins, bleeding esophageal varices, mucosal varicosities, and other similar surgical procedures.[20−23] This is quite curious taking into account that ILs' research is looking for effective pharmaceutical applications, up to now with limited success.[24]

These ionic liquids with long alkyl chains and their mixtures, as happens to other surfactant compounds, present thermotropic and lyotropic liquid crystalline stable mesophases,[25−31] respectively, associated to complex rheologic behaviors, often characterized by non-Newtonian flows and specific viscoelasticities[32−34] that are characteristics that are so far poorly exploited. Because of their amphiphilic and asymmetric nature, such PILs can organize themselves in oriented crystalline matrices above the melting temperature, despite presenting liquid flow properties, and are thus able to be used as supporting media for chemical reactions, development of self-assembling drug delivery systems, materials for membrane separation processes, or electrical conducting media.[35,36]

This work aims at the characterization of the rheologic and thermotropic behavior of four protic ionic liquid and the solid–liquid equilibrium of the binary mixtures of their precursors: oleic acid + monoethanolamine, oleic acid + diethanolamine, stearic acid + monoethanolamine, and stearic acid + diethanolamine. These compounds were chosen because of the sustainable character of fatty acids, and despite the use of ethanolamine soaps in commercial products, these systems have not been previously investigated in the literature. This choice of systems allows the characterization of the effects of molecular structure, alkyl chain length, and presence of unsaturation in the thermodynamic and rheological behavior of these systems and the protic ionic liquids that they originate.

■ EXPERIMENTAL SECTION

Materials. Oleic acid, stearic acid, monoethanolamine, and diethanolamine were supplied by Sigma-Aldrich (St. Louis, MO) with purities greater than 99%. Samples of approximately 1.0 g of oleic

acid + monoethanolamine, oleic acid + diethanolamine, stearic acid + monoethanolamine, and stearic acid + diethanolamine systems were prepared gravimetrically on flasks using an analytical balance (Mettler Toledo, Inc., Columbus, OH) with a precision of $\pm 2 \times 10^{-4}$ g and concentration of component 1 varying from $x_1 = (0.0 \text{ to } 1.0)$ molar fractions for the complete description of the phase diagrams. The mixtures were stirred at 10 K above the mesophases domain of the samples in an oil bath and under injection of nitrogen to avoid oxidation of the compounds. The uncertainty σ_x of the compositions x_1, obtained by error propagation from the values of the weighed masses, was estimated as $\sigma_x = 5 \times 10^{-4}$ (molar fraction).

Differential Scanning Calorimetry (DSC). The solid–liquid equilibrium (SLE) data of the mixtures were characterized using a DSC8500 calorimeter (PerkinElmer, Waltham, MA) previously calibrated with indium (PerkinElmer, Waltham), naphthalene, and cyclohexane (Merck, Whitehouse Station, NJ) at ambient pressure $p = (102.0 \pm 0.5)$ kPa. The samples were submitted to a cooling–heating cycle at 1 K min^{-1} based on a methodology established for measuring of the SLE of fatty systems.[37,38] The temperatures of the thermal transitions were then analyzed in the last heating run and taken as the peak top temperatures. The uncertainty of the temperature was $\sigma_T = 0.40$ K, and this value was obtained by the average of the standard deviation obtained by triplicates of melting temperature values of the pure compounds and mixtures of them.

Light-Polarized Optical Microscopy (POM). The melting profile of the liquid crystalline mesophases of the mixtures were evaluated using a BX51 Olympus polarized optical microscope (Olympus Co., Tokyo, Japan) equipped with a LTS120 Linkam temperature-controlled stage (Linkam Scientific Instruments, Ltd., Tadworth, U.K.) that in this study operated between 243.15 and 393.15 K. Samples (2 mg, approximately) were put in concave slides with coverslips, cooled to 243.15 K, and allowed to stay at this temperature for 30 min. After this, the samples were observed in a 0.1 K min^{-1} heating run. The uncertainty of the temperature obtained from POM measurements was taken as not higher than $\sigma_{POM} = 1.0$ K. The value was estimated by the mean standard deviation obtained by triplicate evaluation of some of the binary mixtures.

Density, Viscosity, and Critical Micellar Concentration (CMC) Measurements. Density and dynamic viscosity measurements of the mixtures were performed between 288.15 and 373.15 K using an automated SVM 3000 Anton Paar rotational Stabinger viscometer-densimeter (Anton Paar, Graz, Austria) as described elsewhere.[39] The relative uncertainty for the dynamic viscosity was 0.35%, and absolute uncertainty for density was 5×10^{-4} g cm^{-3}. CMC measurements of the protic ionic liquids were performed by conductivity using a Mettler-Toledo SevenMulti pHmeter/Conductivimeter (Mettler Toledo Inc., Columbus, OH). Aqueous mixtures of approximately 10^{-3} M of each protic ionic liquid were prepared with Millipore water and kept at 298.15 $\pm$ 0.1 K with a thermostatic water bath. Other concentrations were obtained by successive dilution. The values of the CMC were taken as the interceptions of two successive linear behaviors in the conductivity versus concentration plot.
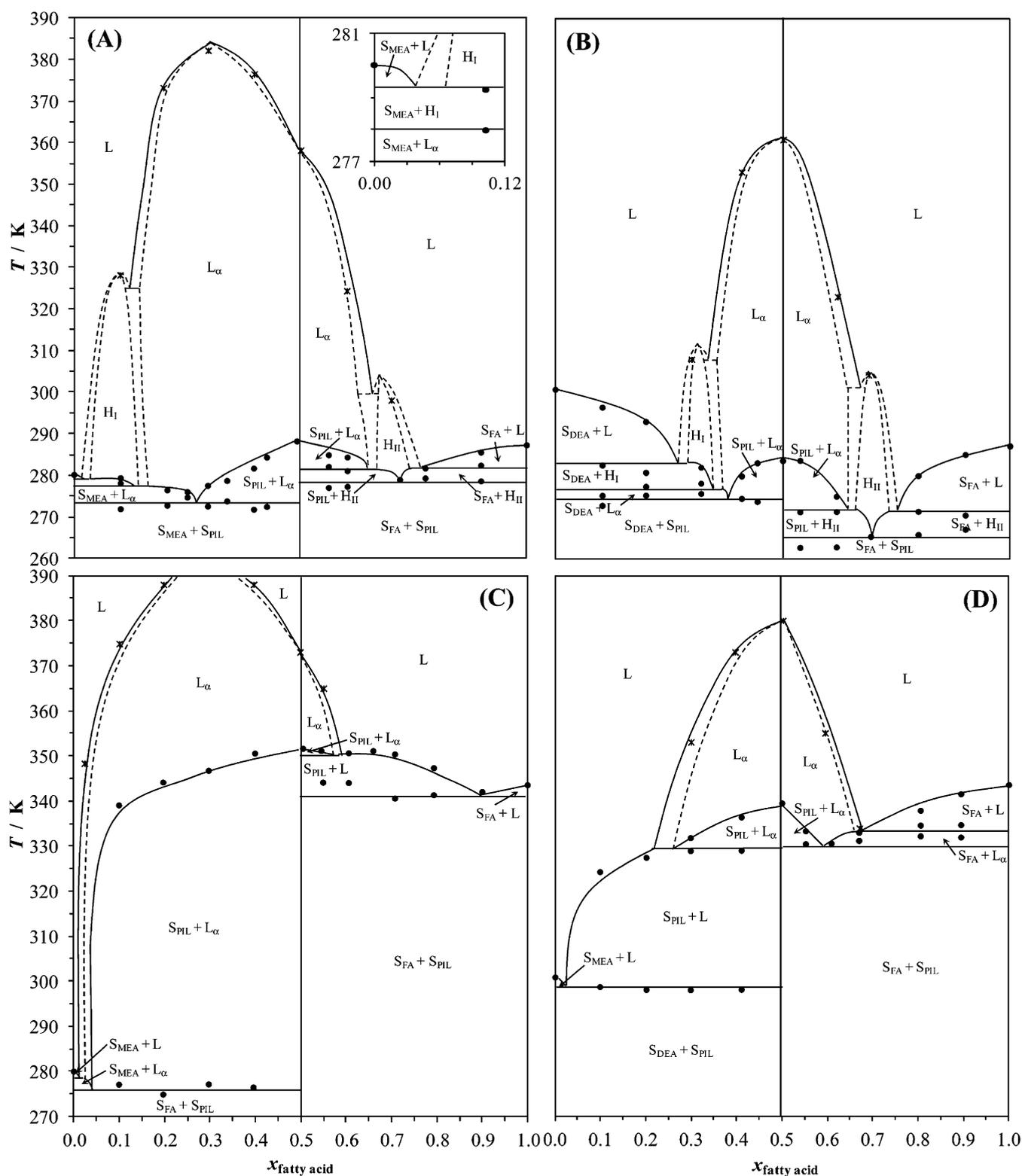
Figure 2. Solid−liquid equilibrium phase diagram of the (A) oleic acid + monoethanolamine, (B) oleic acid + diethanolamine, (C) stearic acid + monoethanolamine, and (D) stearic acid + diethanolamine systems by (●) differential scanning calorimetry and (∗) light-polarized optical microscopy presenting solid monoethanolamine (S_{MEA}), solid diethanolamine (S_{DEA}), solid fatty acid (S_{FA}), solid protic ionic liquid (S_{PIL}), liquid phase (L), normal hexagonal (H_I), lamellar (L_α), and inverted hexagonal (H_{II}) mesophases. Lines are guides for the eyes. Solid lines were experimentally characterized, and dashed lines describe hypothetical phase boundaries based on the Gibbs phase rule.

Rheological Measurements. The stress−strain flow behavior of the protic ionic liquids was determined using a Kinexus-pro stress controlled rotational rheometer (Malvern Instruments Ltd., Worces-

tershire, U.K.). The curves were obtained with a shear rate ranging from 0 to 100 s^{-1} at 298.15−388.15 K using a stainless steel cone and plate geometry with a diameter of 40 mm, angle of 4°, and gap set to

C

dx.doi.org/10.1021/sc400365h | ACS Sustainable Chem. Eng. XXXX, XXX, XXX−XXX
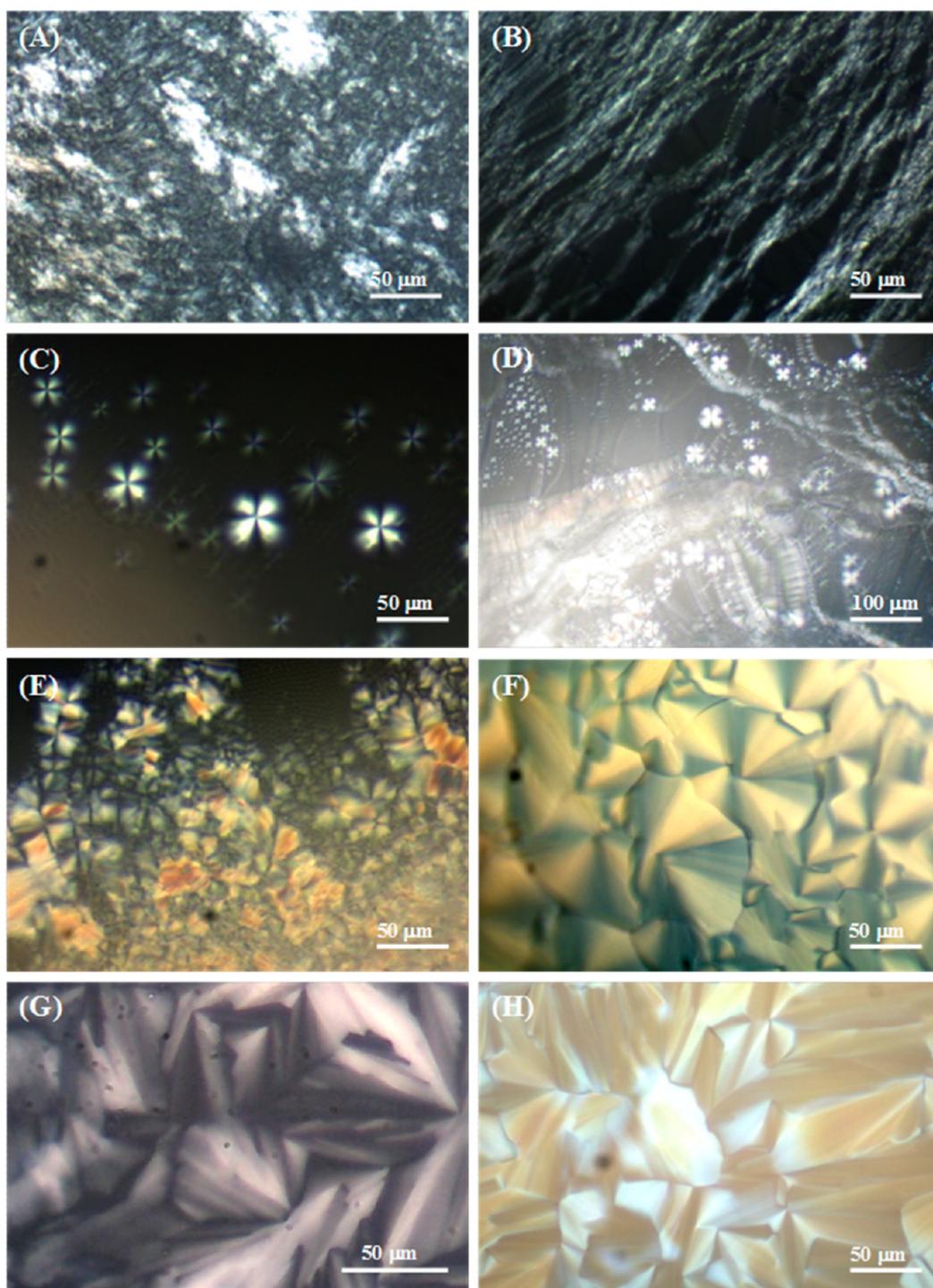
Figure 3. Light-polarized optical micrographs showing the mesophases textures: (A) oily texture in the stearic acid + monoethanolamine at $x_{\text{fatty acid}}$ = 0.2, T = 343.15 K; (B) oily streaks in the oleic acid + diethanolamine at $x_{\text{fatty acid}}$ = 0.6, T = 293.15 K; (C) maltese crosses in an isotropic backgroup oleic acid + diethanolamine at $x_{\text{fatty acid}}$ = 0.5, T = 357.15 K; (D) oily streaks with inserted maltese crosses oleic acid + diethanolamine at $x_{\text{fatty acid}}$ = 0.4, T = 340.15 K, (E) mosaic texture in the stearic acid + monoethanolamine at $x_{\text{fatty acid}}$ = 0.4, T = 363.15 K; and fan-shaped textures in the (F) oleic acid + diethanolamine at $x_{\text{fatty acid}}$ = 0.3, T = 298.15 K; (G) oleic acid + monoethanolamine at $x_{\text{fatty acid}}$ = 0.7, T = 293.15 K; and (H) oleic acid + diethanolamine at $x_{\text{fatty acid}}$ = 0.7, T = 298.15 K.

50 μm. The temperature was controlled ($\pm$0.1 K) by a Peltier system built in the lower fixed flat plate.

■ RESULTS AND DISCUSSION

Phase Behavior. The solid−liquid equilibrium (SLE) phase diagrams of the fatty acid + ethanolamine systems exhibit a

complex multiphasic profile sketched in Figure 2. Experimental SLE data for these systems are reported in the Supporting Information (SI). In all the binary mixtures under study, there is the formation of a protic ionic liquid, i.e., the ethanolammonium salt of a fatty acid, according to the proton transfer reaction sketched in Figure 1, as shown by Alvarez et

al.[12] In fact, at the equimolar composition ($x_1 = 0.5$ molar fraction), the thermogram shows no thermal transitions below the melting temperature, unlike what was observed for the other mixtures, as reported in the experimental data tables in the SI. At this concentration, the system comprises only the pure PIL. Considering the formation of such an intermediate compound, the phase diagrams should be read taking into account two well-defined regions. The left-hand side of the diagram, or the region at $x = 0.0$ to 0.5 fatty acid molar fraction, describes the equilibrium between the ethanolamine and the protic ionic liquid. The right-hand side of the diagram, or the region at $x = 0.5$ to 1.0 fatty acid molar fraction, describes the equilibrium between the protic ionic liquid and the fatty acid. It means that the four solid–liquid phase diagrams here reported display an intermediate compound with a congruent melting profile and thus represent, indeed, eight equilibrium profiles, namely, monoethanolammonium oleate + monoethanolamine, oleic acid + monoethanolammonium oleate, diethanolammonium oleate + diethanolamine, oleic acid + diethanolammonium oleate, monoethanolammonium stearate + monoethanolamine, stearic acid + monoethanolammonium stearate, diethanolammonium stearate + diethanolamine, and stearic acid + diethanolammonium stearate.

These systems present several thermal invariant transitions. In each phase diagram, two of them are related to the eutectic reaction that bounds the solid phase and the other biphasic domains. The first eutectic is observed in the ethanolamine-rich composition region of the diagram and the second in the fatty acid-rich composition region. They are thus related to the minimum point of the *liquidus* line, i.e., the curve that describes the behavior of the melting temperature of the system. The Tammann plots of these invariant transitions are reported in the SI. Their behavior is typically observed for eutectic transitions, with the corresponding enthalpy increasing to the eutectic composition and then decreasing after this transition.[40] These plots suggest that the systems present a full immiscibility in the solid phase because enthalpy is close to zero at pure compound concentration. For stearic acid-based mixtures, the extrapolation of the trend is very close to the pure ethanolamine melting enthalpy value meaning that the eutectic point in such a region is probably very close to pure ethanolamine concentration. The large difference between the pure stearic ionic liquid and pure ethanolamine melting temperatures supports such an evaluation.

Figure 3 presents the principal textures of the lyotropic and thermotropic mesophases (in the case of mixtures or pure PIL at $x_1 = 0.5$, respectively) above the *liquidus* line. Five types of profiles were characterized, those described as oily textures (Figure 3A), oily streaks (Figure 3B), oily streaks with inserted maltese crosses (Figure 3C), maltese crosses in an isotropic background (Figure 3D), and mosaic textures (Figure 3E), related to the appearance of a lamellar mesophase and those with well-defined fan-shaped textures (Figures 3F–H) related to the presence of hexagonal mesophases. These structures are typical of the liquid crystalline state.[26−28,41,42] Well-defined lamellar mesophases were observed in all systems at a particular composition range. Hexagonal mesophases could be clearly observed in the oleic acid-based systems at the extremes of the liquid crystal domain, and this is in agreement with the self-assembly behavior of surfactant molecules. In fact, in aqueous surfactant solutions, hexagonal ensembles are structured at high water concentration, while lamellar matrices appear at intermediate concentrations.[26−28] Thus, considering that the

solute, in this case, is the ethanolamine or the fatty acid, the appearance of hexagonal mesophases before lamellar ones is expected. Moreover, when the ionic liquid is in solution with the ethanolamine, the solvent is hydrophilic. Otherwise, with the fatty acid, the solvent is hydrophobic. Thus, in the ethanolamine-rich region, the hexagonal mesophase observed probably assumes a normal structure, unlike in the fatty acid-rich region where it probably assumes inverted ones. Normal and inverted hexagonal mesophases are known in the literature as type I and II, respectively. It means that, in normal type I hexagonal mesophases, the hydrophilic moiety of the surfactant interacts with the medium, while the hydrophobic moiety is inside of the ensemble. On the other hand, in inverted type II hexagonal mesophases, the opposite structure is observed. Moreover, as previously mentioned, hexagonal mesophases were not observed in the stearic acid-based mixtures. This probably happens because the linear structure of the fatty acid carbon chain prefers to self-assemble in layers instead of cylindrical shapes.[43] This will be further discussed.

Because liquid crystals were not observed in the pure ethanolamines and fatty acids, such structures could be related to the formation of the protic ionic liquids. In fact, oily textures and maltese crosses were clearly observed throughout the liquid crystal phase temperature range at $x = 0.5$ fatty acid molar fraction, i.e., the pure protic ionic liquid. The same textures were reported in the literature for similar compounds.[44−48] They occur due to the amphiphilic nature of the ethanolammonium soap and the complex lyotropic behavior of some of these mixtures, resulting from the different packaging profiles that depend on the polarity of the coexistent compound, either the polar ethanolamine in the ethanolamine-rich composition region or the nonpolar fatty acid in the fatty acid-rich composition region.

Taking into account the existence of these mesophases, it is possible to characterize the other thermal invariant transitions that are observed in the biphasic domain. Oleic acid-based mixtures (Figure 2A and B) present, at the left-hand side of the diagram, two invariant transitions. The first, at a higher temperature, is related to the formation of the hexagonal mesophase, and the second is related to the formation of the lamellar mesophase. In the right-hand side of the diagrams, the ionic liquid-rich region shows one invariant transition related to the lamellar mesophase formation, and the fatty acid-rich region presents one transition, probably related to the formation of the inverted hexagonal mesophase. On the other hand, because stearic acid-based mixtures (Figure 2C and D) showed only lamellar mesophases, the invariant thermal transitions in the biphasic region are related to the formation of such structure.

The profile of the phase diagrams, including the solid–liquid equilibrium and the mesophases, could be sketched in Figure 2A–D, considering the experimental observations and the Gibbs phase rule imposing that at a constant pressure and temperature at most three phases can coexist in a binary mixture.[40,49−51] Taking into account the coexistent phases and mesophases, namely, solid ethanolamine (S_{EA}), solid fatty acid (S_{FA}), solid protic ionic liquid (S_{PIL}), isotropic liquid (L), normal hexagonal (H_I), lamellar (L_α), and inverted hexagonal (H_{II}), it is possible to summarize all biphasic domains that are present in the phase diagrams. In the oleic acid + monoethanolamine (Figure 2A) and oleic acid + diethanolamine (Figure 2B) systems, we have $S_{EA} + S_{PIL}$, $S_{EA} + L_\alpha$, $S_{EA} + H_I$, $S_{EA} + L$, $S_{PIL} + S_{FA}$, $S_{PIL} + L_\alpha$, $S_{PIL} + H_{II}$, $S_{FA} + H_{II}$, and $S_{FA} + L$. In the stearic acid + monoethanolamine system (Figure 2C),

we have $S_{EA} + S_{PIL}$, $S_{EA} + L_{\alpha}$, $S_{EA} + L$, $S_{PIL} + S_{FA}$, $S_{PIL} + L_{\alpha}$, $S_{PIL} + L$, and $S_{FA} + L$. In the stearic acid + diethanolamine system (Figure 2D), we have $S_{EA} + S_{PIL}$, $S_{EA} + L$, $S_{PIL} + L$, $S_{PIL} + S_{FA}$, $S_{PIL} + L_{\alpha}$, $S_{FA} + L_{\alpha}$, and $S_{FA} + L$.

Self-Assembling of PILs. It was mentioned before that the appearance of the liquid crystal mesophases is due to the formation of the protic ionic liquid. In fact, it presents an amphiphilic and asymmetric molecular structure, containing a hydrophilic (ethanolammonium cation) and hydrophobic moiety (fatty acid anion). Such profile characterizes a mesogen, i.e., a compound that under suitable temperature and pressure conditions can build liquid crystal matrices.[36,42] For the understanding of the self-organizing behavior of the protic ionic liquids formed by the reaction of the fatty acids with ethanolamines mixtures, the critical micellar concentration of these compounds in water was measured by conductivity.
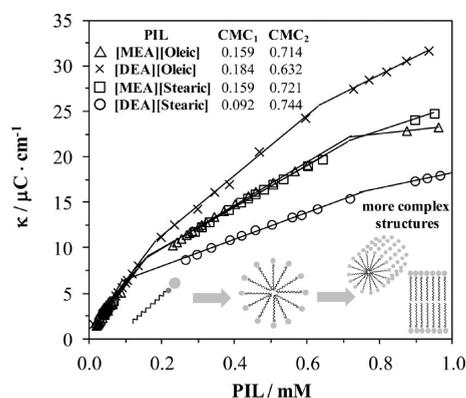

Figure 4. Conductivity (κ) as a function of concentration of protic ionic liquids (PIL) aqueous solutions. Solid lines are linear fitting of the data ($R^2 > 0.98$) for critical micellar concentration determination (CMC).

Figure 4 shows the conductivities of the diluted aqueous solutions of the four protic ionic liquids here studied. As the conductivity increases with the concentration of the ionic liquids in solution, the slope changes defining essentially three different linear regions. Thus, considering that the different dependence of conductivity upon PIL concentration is due to differences in the self-assembly of the mesogens, two CMC values were obtained (as shown in Figure 4). Literature shows that with an increase in the surfactant concentration in aqueous solutions, spherical micelles, cylindrical micelles, or bilayers are formed from the monomers.[52] After the first CMC value, the protic ionic liquid is probably self-assembled in spherical micelles. In fact, taking into account the molecular geometry (local) constraints, the critical packing parameter[53] in all cases assumed values lower than 1/3. This value is related to the formation of spherical micelles with the polar headgroup (ethanolammonium cation) interacting with the aqueous medium (as depicted in Figure 4). Moreover, considering the global constraints imposed by an increase in the concentration of the mixture and intermolecular interactions, the second CMC value could be probably related to the formation of more complex structures, according to similar observations in the literature.[54−56] The formation of such structures is more evident in the oleate ionic liquids because they present a more pronounced shift in the slope and lower CMC_2 values. Assuming, in this case, both global and local constraints, the presence of the unsaturation in the carbon chain of the oleic

ionic liquids might probably favor the formation of cylindrical self-assembling. On the other hand, the geometry of the saturated alkyl chain of the stearic ionic liquids probably led to the formation of bilayer structures. This observation corroborates with the fact that stearic acid based mixtures did not present hexagonal crystals, unlike oleic acid ones, as previously discussed.

Rheological Characterization of PILs and Their Binary Mixtures. Taking into account the organized nature of a liquid crystal microstructure, its properties should present a particular behavior, or even a different profile, when compared with an isotropic media. In fact, visually, some mixtures close to $x = 0.5$ fatty acid molar fraction, including the equimolar concentration, presented a very viscous gel-like behavior. The phase diagrams of the mixtures here studied show that above the *liquidus* line, there is a very large liquid crystalline domain in a broad concentration range and with maximum temperature values close to 390 K. Thus, density and viscosity measurements were determined in order to characterize these fluids, fostering the understanding of the interactions between the compounds in the mixture because in this work the compounds react to form a new substance. Unfortunately, due to their high melting points, the mixtures of stearic acid could not be studied. Figure 5 presents the densities of the oleic acid + monoethanolamine and oleic acid + diethanolamine binary systems from 288.15 to 353.15 K because such mixtures are liquid above 288.15 K. As a first observation, the results seem to be quite trivial with density values at fixed concentrations decreasing linearly ($R^2 \geq 0.99$) with increasing temperature, ranging from $\rho = 1.10$ to 0.85 g cm^{-3}, i.e., from pure ethanolamine to pure oleic acid density values. However, if the density results are seen on their composition dependency at a fixed temperature, the values also decrease with an increase in oleic acid concentration, but a more complex behavior is revealed. Three different regions are now apparent: (1) one in the ethanolamine rich region before the liquid crystal formation, (2) one delimited by the liquid crystal domain (dashed lines of the Figure 5), and (3) one in the fatty acid-rich region where no liquid crystal is observed. These differences in the density result from the peculiar packing profiles that liquid crystals present, which induce changes in the densities of the mixtures. The excess molar volume V^{EX}/cm^3 mol^{-1} data calculated from the experimental density data (Figure 6) are in agreement with the observed nonlinear density dependency and provide further significant details on the molecular interactions. It is important to note that the excess molar volume was calculated considering that at $x = 0.0$ to 0.5 oleic acid molar fraction the mixture is the ethanolamine + ionic liquid binary system and at $x = 0.5$ to 1.0 oleic acid molar fraction the system is the fatty acid + ionic liquid mixture. The results clearly show that, at a fixed temperature, the excess molar volumes of the ethanolamine + protic ionic liquid mixtures present a significant negative deviation from ideal behavior. On the other hand, the excess molar volumes of the oleic acid + protic ionic liquid mixtures present significant positive deviations. Because negative deviations were observed in the first part of the diagram, one can infer that from the point of view of excess molar volumes the interactions between ethanolamine and the ionic liquid are more favorable than the interactions between fatty acid and the ionic liquid. In fact, ethanolamines and fatty acid have quite different size, shape, and polarities. In the ethanolamine + ionic liquid mixture, due to the polar behavior of the ethanolamine, the interactions with the hydrophilic moiety of the ionic liquid
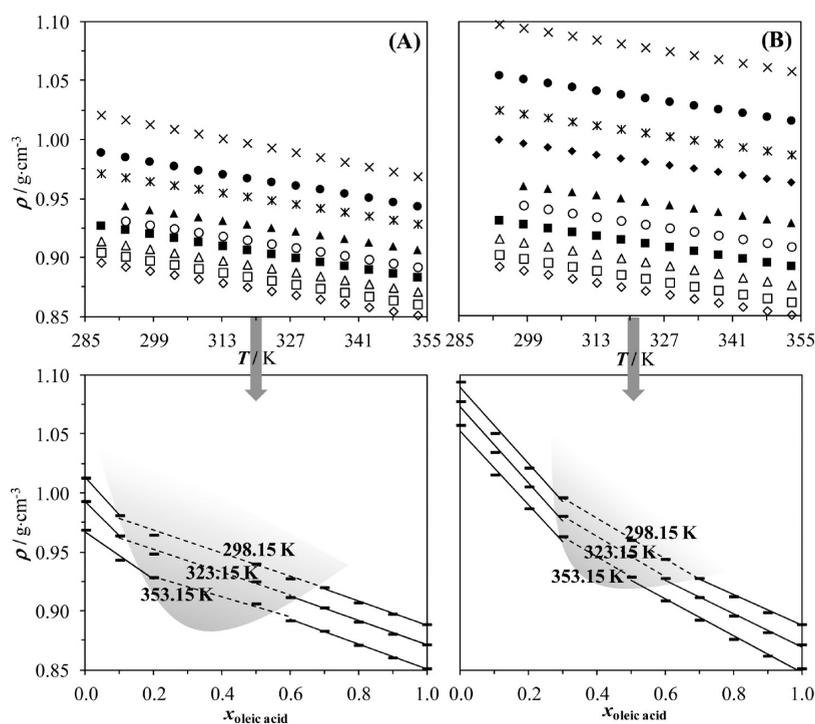
F

dx.doi.org/10.1021/sc400365h | ACS Sustainable Chem. Eng. XXXX, XXX, XXX−XXX

Figure 5. Density data $(\rho/\text{g cm}^{-3})$ as a function of temperature (T/K) for the (A) oleic acid + monoethalonamine and (B) oleic acid + diethanolamine systems at $x_{\text{oleic acid}}$ = 0.0 (×), 0.1 (●), 0.2 (∗), 0.3 (◆), 0.4 (+), 0.5 (▲), 0.6 (○), 0.7 (■), 0.8 (△), 0.9 (□), and 1.0 (◇). At the bottom of each plot are density data as a function of oleic acid molar fraction at 298.15, 323.15, and 353.15 K. Solid and dashed lines are guides for the eyes. Gray regions represent the liquid crystal domain.
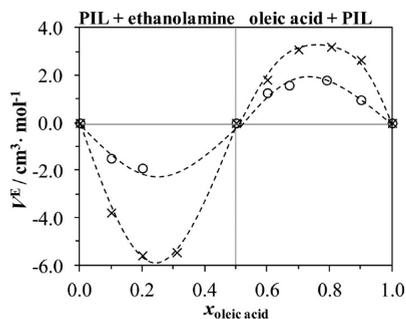

Figure 6. Experimental excess molar volume data of the (○) oleic acid + monoethalonamine and (×) oleic acid + diethanolamine systems at 298.15 K. Dashed lines are guides for the eyes. Vertical gray line at x = 0.5 (pure PIL) depicts the "true" system indicated at the top of the plot.

are preferred. The large size differences may also favor the packing of the ensemble. On the opposite, in the fatty acid + ionic liquid systems, the interactions with the hydrophobic moiety of the ionic liquid are preferred due to the apolar behavior of the organic acid. Thus, the rigid structure of the liquid crystal formed and the large size of the long carbon chain probably do not allow much possibilities of packing leading to positive deviations from ideal behavior.

Figure 7 shows the dynamic viscosity measurements for the same systems from 288.15 to 358.15 K except at and close to the equimolar composition for the oleic acid + monoethanolamine system due to its high viscosity with a gel-like behavior. In the case of pure PILs, shear rate-dependent rheological measurements were conducted and will be later discussed. An exponential decay of the viscosity with temperature was observed, being more pronounced close to the pure ionic

liquid. This is clearly visible considering the isothermal behavior at 353.15 K of the viscosity with the fatty acid concentration at the bottom of Figure 7. The viscosity values increased with the concentration from pure ethanolamine composition to the protic ionic liquid, and then they start to decrease again to the value of pure oleic acid. Another singular behavior from the viscosity measurements can be highlighted if the data is fitted to an Arrhenius-like exponential equation (eq 1)

$$\ln(\eta) = \ln(A) + \frac{E_A}{RT} \tag{1}$$

where η is the dynamic viscosity (Pa s), E_A is the activation energy (J mol^{-1}), R is the gas constant (8.314 J mol^{-1} K^{-1}), T is temperature (K), and A is the pre-exponential factor (Pa s). Thence, Figure 8 shows the logarithm of the viscosity data, ln (η), as a function of T^{-1}. The fitting procedure, which is presented at the right side of Figure 8, shows that the trend presents a shift with a significant change in the activation energy E_A at a temperature $(T_{\text{inters}}$ in Figure 8) close to the melting of the mesophases. Considering the meaning of the coefficients of the Arrhenius equation, the results reveal that the activation energy of the liquid crystalline state is higher than that in the isotropic liquid phase. The crystalline mesophase needs, thus, more energy to flow than the isotropic liquid.[57]

Figure 9 shows some of the flow curves of the oleate-based PILs (x = 0.5 oleic acid molar fraction) at 293.15 to 363.15 K, describing the shear rate-dependence of the samples' shear stresses. For the monoethanolammonium oleate sample at $T >$ 348.15 K, the shear rate is directly proportional to the shear stress, with no evidence of yield stress (σ_0), characterizing a clear Newtonian behavior (eq 2). The same result is observed for diethanolammonium oleate samples at $T >$ 323.15 K. Below such temperature values, for both PILs, the increase in shear
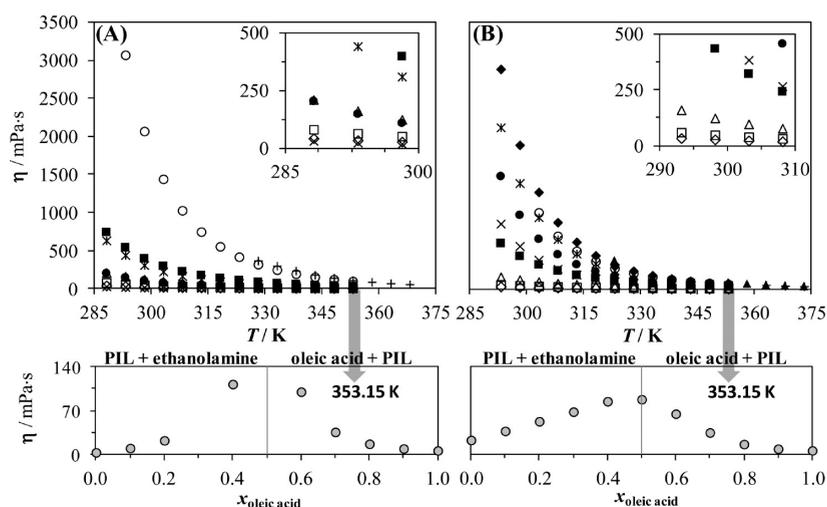
Figure 7. Dynamic viscosity data of (A) oleic acid + monoethanolamine and (B) oleic acid + diethanolamine at $x_{oleic\ acid}$ = 0.0 ($\times$); 0.1 ($\bullet$); 0.2 ($*$); 0.3 ($\blacklozenge$); 0.4 (+); 0.5 ($\blacktriangle$); 0.6 ($\bigcirc$); 0.7 ($\blacksquare$); 0.8 ($\triangle$); 0.9 ($\square$); 1.0 ($\lozenge$). Details at the top right of the plots show magnifications of the data at low η values. At the bottom of each plot are viscosity data as a function of fatty acid molar fraction at 353.15 K. Vertical gray lines at x = 0.5 (pure PIL) depict the "true" systems indicated above.
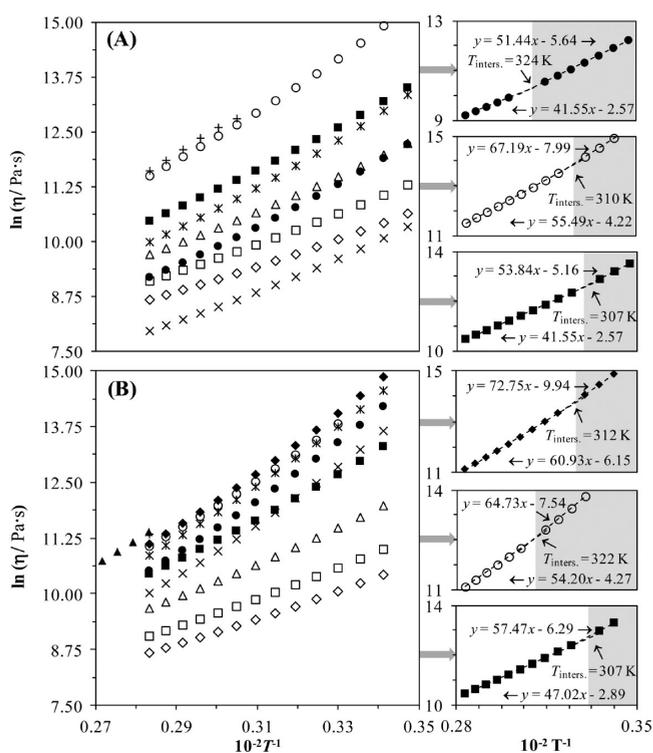

Figure 8. Linearization procedure of the dynamic viscosity η data using the Arrhenius-like eq 1. (A) Oleic acid + monoethanolanmine and (B) oleic acid + diethanolamine at $x_{oleic\ acid}$ = 0.0 ($\times$); 0.1 ($\bullet$); 0.2 ($*$); 0.3 ($\blacklozenge$); 0.4 (+); 0.5 ($\blacktriangle$); 0.6 ($\bigcirc$); 0.7 ($\blacksquare$); 0.8 ($\triangle$); 0.9 ($\square$); 1.0 ($\lozenge$). At the right of each plot are linear fittings of the data (R^2 > 0.99) at some concentrations. Gray regions represent the liquid crystal domain.

rates leads to a nonlinear increase in shear stress. At 298.15 $\leq$ T $\leq$ 348.15 K, the monoethanolammonium oleate sample presented a significant yield stress (outlined by the dashed circles in Figure 9), whose values increase with an decrease in temperature from σ_0 = 10 to 70 Pa. At this range, the shear rate/shear stress dependence changes gradually to a marked nonlinear behavior that could be adjusted by the Vocadlo

model[58,59] (eq 3) up to T > 293.15 K. At this low temperature, the yield stress increases to σ_0 > 200 Pa with a linear dependence between shear rate and shear stress such that the flow curve is well-characterized by the Bingham plastic model (eq 4, R^2 > 0.99). Comparatively, the non-Newtonian temperature domain of the diethanolammonium oleate samples did not present yield stress up to 308.15 K, where the flow curve is well adjusted (R^2 > 0.99) by a shear-thinning profile (eq 5). However, with the temperature decreasing (T < 308.15 K), the flow curve presents a yield stress, and the Herschel-Bulkley model (eq 6) could be accurately adjusted (R^2 > 0.95). The model's parameters fitted to flow experimental data are in the SI. The flow models adopted here[60] can be described as follows

$$\sigma = \eta\dot{\gamma} \tag{2}$$

$$\sigma = (\sigma_{0V}^{1/n_v} + K_V\dot{\gamma})^{n_V} \tag{3}$$

$$\sigma = \sigma_0 + \eta'\dot{\gamma} \tag{4}$$

$$\sigma = K\dot{\gamma}^n \tag{5}$$

$$\sigma = \sigma_{0H} + K_H\dot{\gamma}^{n_H} \tag{6}$$

where σ is the shear stress (Pa), η is the viscosity (Pa s), $\dot{\gamma}$ is the shear rate (s^{-1}), σ_0, σ_{0V}, and σ_{0H} are the yield stresses (Pa) related to each model, K, K_V and K_H are the consistency indexes related to each model, η' is the Bingham plastic viscosity, n, n_V, and n_H are flow behavior indexes related to each model, and the subscripts V and H make reference to the Vocadlo and Herschel–Bulkley models, respectively. The non-Newtonian behavior displayed by these PILs is thus a unique characteristic of these compounds, and the flow phenomena here observed play a key role in numerous industry applications.[32−36,57] The self-assembly ability of the PILs and formation of thermotropic mesophases with bilayered lamellar-oriented structures above the melting point are the main reason for the non-Newtonian rheological behavior here described. Moreover, the chemical interactions among the molecules appear to be strong enough for the requirement of a critical shear stress. The increasing temperatures lead to a decrease in the apparent viscosity. This,
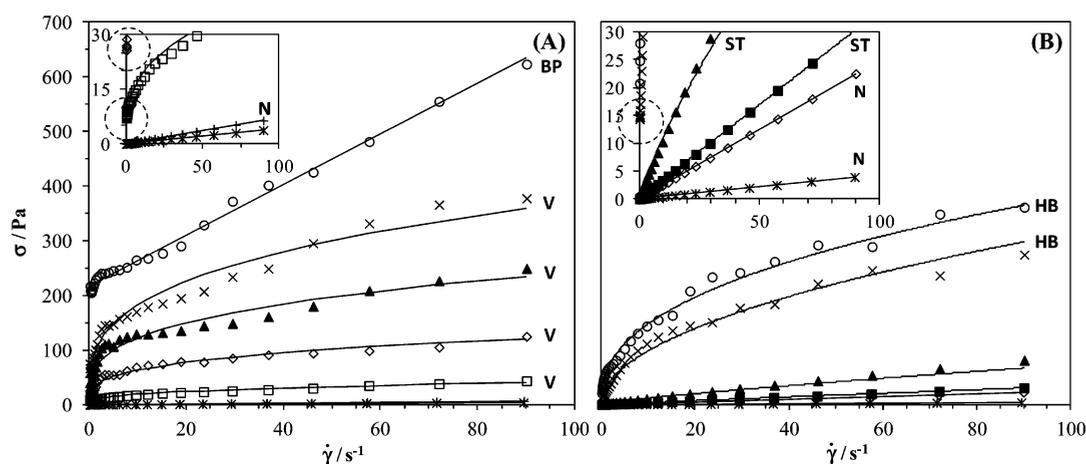
H

dx.doi.org/10.1021/sc400365h | ACS Sustainable Chem. Eng. XXXX, XXX, XXX−XXX

Figure 9. Shear stress (σ) versus shear rate ($\dot{\gamma}$) curves of (A) monoethanolammonium oleate and (B) diethanolammonium oleate at 293.15 (○), 298.15 (×), 308.15 (▲), 323.15 (■), 328.15 (◇), 348.15 (□), 353.15 (+), and 363.15 (✳) K. Solid lines are fitted curves. Labels **N**, **ST**, **V**, **BP**, and **HB** stand for Newtonian, shear-thinning, Vocadlo, Bingham plastic, and Herschel−Bulkley models, respectively.

for practical purposes, says there is an attenuation of the non-Newtonian behavior followed by the appearance of a Newtonian profile at sufficiently high temperatures. The temperature increase induces the breaking of the interactions that support the liquid crystalline microstructure. The concentration of the isotropic phase increases with depletion of the mesophase, as observed in the phase diagrams (Figure 1) and in the polarized optical micrographs (Figure 2A, typical lamellar texture at low temperatures; Figure 2C, textures at high temperatures). It was also observed that the non-Newtonian behavior of monoethanolammonium oleate is more evident than for the diethanolammonium oleate in special at low temperatures where the elastic characteristic of such PIL follows a Bingham plastic profile, presenting very high yield stresses. So, regarding the size of the cation in the surfactant molecule structure, one might suppose that the bilayers constructed by the monoethanolammonium oleate are more packed with stronger intermolecular hydrogen bonding networks than the diethanolammonium oleate structure, whose larger cation decreases the self-assembly ability. In fact, complex structures are more easily formed by monoethanolammonium oleate due to its lower CMC_2 value. The non-Newtonian behavior exhibited by the ethanolammonium oleates is quite interesting concerning their use in the formulation of products and considering the particular physicochemical properties of the protic ionic liquids for specific applications.[4−6,12,15−17,35,36]

CONCLUSIONS

Four PILs based on oleic and stearic acids, with mono- and di-ethanolamines as cations, and the binary mixtures used for their preparation were here investigated. The protic ionic liquids are shown to display an interesting thermotropic behavior with the formation of lamellar mesophases. The SLE phase diagrams of the mixtures of their precursors display a congruent melting behavior with lamellar and hexagonal lyotropic mesophases. Moreover, the oleic acid-based systems also present a non-Newtonian behavior clearly observed in the flow curves obtained by the stress-controlled rheological assays. Although many ethanolammonium carboxylates have a range of industrial applications known, considering their renewable origin, the novel characteristics here reported, such as the formation of liquid crystalline structures in addition to the non-Newtonian behavior and the unique properties resulting from their ionic

liquid character, confer to the compounds here investigated a great potential. On the basis of these results, numerous applications may be foreseen for these compounds, besides those currently in use, which should be the object of future studies.

ASSOCIATED CONTENT

ⓢ Supporting Information

Tables with experimental solid−liquid equilibrium data, Tammann plots of eutectic transitions, and rheological models' parameters fitted to experimental flow curves. This material is available free of charge via the Internet at http://pubs.acs.org.

AUTHOR INFORMATION

Corresponding Author

*Fax: + 351 234 401 470. Tel: + 351 234 401 507. E-mail: jcoutinho@ua.pt.

Notes

The authors declare no competing financial interest.

REFERENCES

(1) Brennecke, J. F.; Maginn, E. J. Ionic liquids: Innovative fluids for chemical processing. *Aiche J.* **2001**, *47* (11), 2384−2389.

(2) Plechkova, N. V.; Seddon, K. R. Applications of ionic liquids in the chemical industry. *Chem. Soc. Rev.* **2008**, *37* (1), 123−150.

(3) Rogers, R. D.; Seddon, K. R. Ionic liquids—Solvents of the future? *Science* **2003**, *302* (5646), 792−793.

(4) Greaves, T. L.; Weerawardena, A.; Krodkiewska, I.; Drummond, C. J. Protic ionic liquids: Physicochemical properties and behavior as amphiphile self-assembly solvents. *J. Phys. Chem. B* **2008**, *112* (3), 896−905.

(5) Greaves, T. L.; Weerawardena, A.; Fong, C.; Krodkiewska, I.; Drummond, C. J. Protic ionic liquids: Solvents with tunable phase behavior and physicochemical properties. *J. Phys. Chem. B* **2006**, *110* (45), 22479−22487.

(6) Belieres, J. P.; Angell, C. A. Protic ionic liquids: Preparation, characterization, and proton free energy level representation. *J. Phys. Chem. B* **2007**, *111* (18), 4926−4937.

(7) Ventura, S. P. M.; Gurbisz, M.; Ghavre, M.; Ferreira, F. M. M.; Gonçalves, F.; Beadham, I.; Quilty, B.; Coutinho, J. A. P.; Gathergood, N. Imidazolium and pyridinium ionic liquids from mandelic acid derivatives: Synthesis and bacteria and algae toxicity evaluation. *ACS Sustainable Chem. Eng.* **2013**, *1* (4), 393−402.

(8) Handy, S. T. Greener solvents: Room temperature ionic liquids from biorenewable sources. *Chem.—Eur. J.* **2003**, *9* (13), 2938−2944.

(9) Hou, X.-D.; Li, N.; Zong, M.-H. Facile and simple pretreatment of sugar cane bagasse without size reduction using renewable ionic liquids−water mixtures. *ACS Sustainable Chem. Eng.* **2013**, *1* (5), 519−526.

(10) FAO Agricultural Outlook, 2013. FAO OECD. http://www.fao.org.

(11) Chu, Z.; Feng, Y. Vegetable-derived long-chain surfactants synthesized via a "green" route. *ACS Sustainable Chem. Eng.* **2012**, *1* (1), 75−79.

(12) Alvarez, V. H.; Mattedi, S.; Martin-Pastor, M.; Aznar, M.; Iglesias, M. Synthesis and thermophysical properties of two new protic long-chain ionic liquids with the oleate anion. *Fluid Phase Equilib.* **2010**, *299* (1), 42−50.

(13) Reinish, M. D. Soaps from fatty acids. *J. Am. Oil Chem. Soc.* **1952**, *29* (11), 506−510.

(14) Maag, H. Fatty-acid derivatives: Important surfactants for household, cosmetic and industrial purposes. *J. Am. Oil Chem. Soc.* **1984**, *61* (2), 259−267.

(15) de Souza, R. L.; de Faria, E. L. P.; Figueiredo, R. T.; Freitas, L.; Iglesias, M.; Mattedi, S.; Zanin, G. M.; dos Santos, O. A. A.; Coutinho, J. A. P.; Lima, Á. S.; Soares, C. M. F. Protic ionic liquid as additive on lipase immobilization using silica sol−gel. *Enzyme Microb. Technol.* **2013**, *52* (3), 141−150.

(16) Trusler, R. B. Ethanolamine soaps. *Ind. Eng. Chem.* **1929**, *21*, 685−687.

(17) Zhu, S.; Heppenstall-Butler, M.; Butler, M. F.; Pudney, P. D. A.; Ferdinando, D.; Mutch, K. J. Acid soap and phase behavior of stearic acid and triethanolamine stearate. *J. Phys. Chem. B* **2005**, *109* (23), 11753−11761.

(18) Zhu, S.; Pudney, P. D. A.; Heppenstall-Butler, M.; Butler, M. F.; Ferdinando, D.; Kirkland, M. Interaction of the acid soap of triethanolamine stearate and stearic acid with water. *J. Phys. Chem. B* **2007**, *111* (5), 1016−1024.

(19) Pudney, P. D. A.; Mutch, K. J.; Zhu, S. P. Characterising the phase behaviour of stearic acid and its triethanolamine soap and acid-soap by infrared spectroscopy. *Phys. Chem. Chem. Phys.* **2009**, *11* (25), 5010−5018.

(20) Meyer, N. E. Monoethanolamine oleate: A new chemical for the obliteration of varicose veins. *Am. J. Surg.* **1938**, *40* (3), 628−629.

(21) Yamamoto, K.; Sakaguchi, H.; Anai, H.; Tanaka, T.; Morimoto, K.; Kichikawa, K.; Uchida, H. Sclerotherapy for simple cysts with use of ethanolamine oleate: Preliminary experience. *Cardiovasc. Inter. Rad.* **2005**, *28* (6), 751−755.

(22) Kiripolsky, M. G. Commentary: More on ethanolamine oleate as a vascular sclerosant. *Dermatol. Surg.* **2010**, *36* (7), 1153−1154.

(23) Gomes, C. C.; Gomez, R. S.; do Carmo, M. A.; Castro, W. H.; Gala-Garcia, A.; Mesquita, R. A. Mucosal varicosities: Case report treated with monoethanolamine oleate. *Med. Oral Patol. Oral Cir. Bucal.* **2006**, *11* (1), E44−E46.

(24) Hough, W. L.; Smiglak, M.; Rodriguez, H.; Swatloski, R. P.; Spear, S. K.; Daly, D. T.; Pernak, J.; Grisel, J. E.; Carliss, R. D.; Soutullo, M. D.; Davis, J. J. H.; Rogers, R. D. The third evolution of ionic liquids: Active pharmaceutical ingredients. *New J. Chem.* **2007**, *31* (8), 1429−1436.

(25) Greaves, T. L.; Weerawardena, A.; Fong, C.; Drummond, C. J. Formation of amphiphile self-assembly phases in protic ionic liquids. *J. Phys. Chem. B* **2007**, *111* (16), 4082−4088.

(26) Lawrence, M. J. Surfactant systems: Their use in drug-delivery. *Chem. Soc. Rev.* **1994**, *23* (6), 417−424.

(27) Sagar, G. H.; Arunagirinathan, M. A.; Bellare, J. R. Self-assembled surfactant nano-structures important in drug delivery: A review. *Indian J. Exp. Biol.* **2007**, *45* (2), 133−159.

(28) Muller-Goymann, C. C. Physicochemical characterization of colloidal drug delivery systems such as reverse micelles, vesicles, liquid crystals and nanoparticles for topical administration. *Eur. J. Pharm. Biopharm.* **2004**, *58* (2), 343−356.

(29) Bowlas, C. J.; Bruce, D. W.; Seddon, K. R. Liquid-crystalline ionic liquids. *Chem. Commun.* **1996**, *14*, 1625−1626.

(30) Holbrey, J. D.; Seddon, K. R. The phase behaviour of 1-alkyl-3-methylimidazolium tetrafluoroborates; ionic liquids and ionic liquid crystals. *J. Chem. Soc., Dalton Trans.* **1999**, *13*, 2133−2139.

(31) Li, X.-W.; Zhang, J.; Dong, B.; Zheng, L.-Q.; Tung, C.-H. Characterization of lyotropic liquid crystals formed in the mixtures of 1-alkyl-3-methylimidazolium bromide/p-xylene/water. *Colloids Surf., A* **2009**, *335* (1−3), 80−87.

(32) Burrell, G. L.; Dunlop, N. F.; Separovic, F. Non-Newtonian viscous shear thinning in ionic liquids. *Soft Matter* **2010**, *6* (9), 2080−2086.

(33) Amann, T.; Dold, C.; Kailer, A. Rheological characterization of ionic liquids and ionic liquid crystals with promising tribological performance. *Soft Matter* **2012**, *8* (38), 9840−9846.

(34) Mukherjee, I.; Manna, K.; Dinda, G.; Ghosh, S.; Moulik, S. P. Shear- and temperature-dependent viscosity behavior of two phosphonium-based ionic liquids and surfactant Triton X-100 and their biocidal activities. *J. Chem. Eng. Data* **2012**, *57* (5), 1376−1386.

(35) Binnemans, K. Ionic liquid crystals. *Chem. Rev.* **2005**, *105* (11), 4148−4204.

(36) Gin, D. L.; Pecinovsky, C. S.; Bara, J. E.; Kerr, R. L. Functional lyotropic liquid crystal materials. *Struct. Bonding (Berlin)* **2008**, *128*, 181−222.

(37) Costa, M. C.; Rolemberg, M. P.; Boros, L. A. D.; Krahenbuhl, M. A.; de Oliveira, M. G.; Meirelles, A. J. A. Solid-liquid equilibrium of binary fatty acid mixtures. *J. Chem. Eng. Data* **2007**, *52* (1), 30−36.

(38) Maximo, G. J.; Costa, M. C.; Meirelles, A. J. A. Solid−liquid equilibrium of triolein with fatty alcohols. *Braz. J. Chem. Eng.* **2013**, *30* (1), 33−43.

(39) Carvalho, P. J.; Regueira, T.; Santos, L. M. N. B. F.; Fernandez, J.; Coutinho, J. A. P. Effect of water on the viscosities and densities of 1-butyl-3-methylimidazolium dicyanamide and 1-butyl-3-methylimida-zolium tricyanomethane at atmospheric pressure. *J. Chem. Eng. Data* **2010**, *55* (2), 645−652.

(40) Chernik, G. G. Phase-equilibria in phospholipid water-systems. *Adv. Colloid Interface Sci.* **1995**, *61*, 65−129.

(41) Greaves, T. L.; Weerawardena, A.; Fong, C.; Drummond, C. J. Many protic ionic liquids mediate hydrocarbon-solvent interactions and promote amphiphile self-assembly. *Langmuir* **2007**, *23* (2), 402−404.

(42) Dierking, I. *Textures of Liquid Crystals*; Wiley-VCH: Weinheim, 2003.

(43) Novales, B.; Navailles, L.; Axelos, M.; Nallet, F.; Douliez, J.-P. Self-assembly of fatty acids and hydroxyl derivative salts. *Langmuir* **2008**, *24* (1), 62−68.

(44) Sagnella, S. M.; Conn, C. E.; Krodkiewska, I.; Moghaddam, M.; Drummond, C. J. Endogenous nonionic saturated monoethanolamide lipids: Solid state, lyotropic liquid crystalline, and solid lipid nanoparticle dispersion behavior. *J. Phys. Chem. B* **2010**, *114* (4), 1729−1737.

(45) Sagnella, S. M.; Conn, C. E.; Krodkiewska, I.; Drummond, C. J. Nonionic diethanolamide amphiphiles with saturated hydrocarbon chains: Neat crystalline and lyotropic liquid crystalline phase behavior. *J. Colloid Interface Sci.* **2012**, *385* (1), 87−95.

(46) Sagnella, S. M.; Conn, C. E.; Krodkiewska, I.; Drummond, C. J. Nonionic diethanolamide amphiphiles with unsaturated C18 hydro-carbon chains: Thermotropic and lyotropic liquid crystalline phase behavior. *Phys. Chem. Chem. Phys.* **2011**, *13* (29), 13370−13381.

(47) Fay, H.; Meeker, S.; Cayer-Barrioz, J.; Mazuyer, D.; Ly, I.; Nallet, F.; Desbat, B.; Douliez, J.-P.; Ponsinet, V.; Mondain-Monval,

O. Polymorphism of natural fatty acid liquid crystalline phases. *Langmuir* **2011**, *28* (1), 272−282.

(48) Zheng, M.; Wang, Z.; Liu, F.; Mi, Q.; Wu, J. Study on the microstructure and rheological property of fish oil lyotropic liquid crystal. *Colloids Surf., A* **2011**, *385* (1−3), 47−54.

(49) Reid, R. C.; Prausnitz, J. M.; Pouling, B. E. *The Properties of Gases and Liquids*; McGraw-Hill: New York, 1987.

(50) Laughlin, R. G. *The Aqueous Phase Behavior of Surfactants*; Academic Press: London, 1994.

(51) Chernik, G. G. A differential scanning calorimetry study of a binary-system 0.1. Interpretation of DSC curves for isothermal and nonisothermal phase-transitions in binary-systems. *J. Colloid Interface Sci.* **1991**, *141* (2), 400−408.

(52) Figueira-Gonzalez, M.; Francisco, V.; Garcia-Rio, L.; Marques, E. F.; Parajo, M.; Rodriguez-Dafonte, P. Self-aggregation properties of ionic liquid 1,3-didecyl-2-methylimidazolium chloride in aqueous solution: From spheres to cylinders to bilayers. *J. Phys. Chem. B* **2013**, *117* (10), 2926−2937.

(53) Hyde, S.; Andersson, S.; Larsson, K.; Blum, Z.; Landh, T.; Lidin, S.; Ninham, B. W. *The Language of Shape − The Role of Curvature in Condensed Matter: Physics, Chemistry and Biology*; Elsevier Science B.V.: Amsterdam, 1997.

(54) Kucharski, S. Surface properties and micelle formation of n,n-di-(2-hydroxy-3-alkoxypropyl)ethanolamine and n-(2-hydroxy-3-alkoxypropyl)diethanolamine surfactants. *J. Colloid Interface Sci.* **1978**, *64* (2), 300−310.

(55) Malik, W. U.; Chand, P. Critical micelle concentration of lauric acid-diethanolamine condensate by polarographic and spectrophotometric methods: A comparative study. *J. Am. Oil Chem. Soc.* **1966**, *43* (7), 446−&.

(56) Mukherjee, P.; Dash, S.; Patel, S.; Mishra, B. K. Self-organized assemblies of surfactants derived from ethanolamines. *J. Dispersion Sci. Technol.* **2012**, *33* (6), 881−886.

(57) Weiss, R. G. Thermotropic liquid crystals as reaction media for mechanistic investigations1. *Tetrahedron* **1988**, *44* (12), 3413−3475.

(58) Rao, M. A. *Rheology of Fluid and Semisolid Foods*; Springer: New York, 2007.

(59) Vocadlo, J. J.; MooYoung, M. Rheological properties os some commercially available fats. *Can. Inst. Food Technol. J.* **1969**, *2*, 137−140.

(60) Rao, M. A. Rheology of liquid foods: A review. *J. Texture Stud.* **1977**, *8* (2), 135−168.